Investigation of the Superconducting-Energy-Gap Behavior of Single-Crystal Rhenium by Tunneling*

S. I. Ochiai
Welding Laboratory, University of Osaka, Osaka, Japan
and
M. L. A. MacVicar
Department of Physics, Massachusetts Institute of Technology, Cambridge, Massachusetts 02139
and
R. M. Rose
Department of Metallurgy and Materials Science, Massachusetts Institute of Technology, Cambridge, Massachusetts 02139
(Received 4 June 1971)

A 15.7% anisotropy in the superconducting energy gap has been measured by electron tunneling into single crystals of rhenium, using thin carbon films as the tunneling barrier to form Re-C-In sandwiches. The energy-gap behavior vs temperature is BCS-like. The anisotropy agrees with ultrasonic measurements of other hcp metals and suggests that phonon dispersion plays a dominating role in the gap behavior. However, gap values determined from *multiparticle* tunneling data exhibited reduced gap magnitudes and a dissimilar crystallographic behavior.

I. INTRODUCTION

We present here the first known tunneling measurements on superconducting rhenium single crystals. Fabrication of oxide-barrier tunneling junctions is difficult because the oxides which form on the surface of rhenium do not insulate. Using an evaporated layer of noncrystalline carbon as a tunneling barrier, we have measured the anisotropy of Δ_{Re} in rhenium-carbon-indium junctions. Although the quality of the I-V characteristics of such junctions is inferior to those obtainable with superconductors that oxidize, the data were more than suitable for determining the energy-gap behavior, thus providing information helpful to determining whether the electronic structure or the crystal lattice dominates gap anisotropy.

II. BACKGROUND

A. Superconductivity

In 1959, Morse, Olsen, and Gavenda[1] observed by ultrasonic attenuation measurements on single-crystal tin that $2\Delta_{(0)}/kT_c$ varied from 3.2 to 4.3. Since then, anistropy in the superconducting energy gap has been observed in several metals. Table I lists some of these measurements. Temperature-dependence observations often show significant deviations from BCS behavior. The basis of such non-BCS[9] behavior lies in the nature of the electron-phonon coupling. It is not clearly understood whether the electronic band structure of a superconducting metal, or the phonon-spectrum distribution, is the dominating influence in determining the anisotropy. Zavaritskii attempted to correlate multitudinous energy-gap data obtained by tunneling measurements on single crystals of tin to the known Fermi-surface topology of that metal.[10] In some cases, Δ values relatively constant in magnitude existed across a region corresponding to a particular sheet of Fermi surface, and indications of magnitude change were seen at the boundary. Zavaritskii concluded that such behavior was consistent with the electronic structure being responsible for anisotropy in Δ. For crystallographic directions thought to have more than one sheet of the Fermi surface contributing to the tunneling current, Zavaritskii observed more than one gap value.

Bennett, assuming that anisotropy in the phonon spectrum is responsible for the behavior of Δ, was able to calculate expected values of Δ assuming a simple harmonic expansion of the phonon function according to crystal symmetry.[11] These values were in good agreement with Zavaritskii's data. By a similar calculation carried out for tunneling data obtained by Rochlin[12] on polycrystalline lead films, Bennett showed that Δ values obtained by assuming the main source of anisotropy to be in the phonon spectrum itself were in excellent agreement with experiment.[13] Lead has long been observed to be strongly non-BCS-like in its gap behavior, with $2\Delta_{(0)}/kT_c$ as large as 4.4, indicating retardation effects and damping effects due to a strong phonon coupling. Recent gap measurements by Blackford and March,[14] however, show gap behavior for single-crystal lead unlike that observed by Rochlin, and seemingly unexplained.

TABLE I. Energy-gap anisotropy in various metals of single-crystal form.

Element	Direction of sampling	$2\Delta_{(0)}/kT_c$	Method	Crystal structure	Ref.
Nb	[111]	3.60±0.1	ultra-	bcc	2
	[110]	3.55±0.1	sonics		
	[100]	3.35±0.1			
Nb	[111]	4.02±1%	tunnel-	bcc	16, 17
	[110]	3.91±1%	ing		
	[100]	3.59±1%			
Ta	[110]	3.5±0.1	ultra-	bcc	3
			sonics		
V	[110]	3.4±0.2	ultra-	bcc	4
	[111]	3.2±0.2	sonics		
	[100]	3.1±0.2			
V	[110]	3.5±0.1	ultra-	bcc	3
			sonics		
Mo	[100]	3.5±0.2	ultra-	bcc	5
			sonics		
Al	[100]	3.7±0.3	ultra-	fcc	6
			sonics		
Pb	[101]	4.00 (4.45) ±1%	tunnel-	fcc	14
			ing		
	[001]	3.93 (4.42) ±1%			
	[111]	3.80 (4.48) ±1%			
Sn	[110]	3.8±0.1	ultra-	bct	15
	[100]	3.5±0.2	sonics		
	[001]	3.1±0.1			
Sn	[110]	3.8±0.1	ultra-	bct	1
	[100]	3.5±0.1	sonics		
	[001]	3.2±0.1			
Sn	[001]	4.3 (3.7 ~3.8*)	tunnel-	bct	10
			ing		
	[110]	3.7~3.8			
	[100]	3.7~3.8 (3.1*)			
Ga	[010]	3.9	ultra-	rhomb.	7
	[001]	3.5	sonics		
Ga	[010]	3.78	tunnel-	rhomb.	8
	[110]	3.78~3.63	ing		
	[001]	3.63			
Zn	[$1\bar{2}10$]	3.8±0.2	ultra-	hcp	4
	[$10\bar{1}0$]	3.4±0.2	sonics		
Zn	[$1\bar{2}10$]	3.64±0.1	ultra-	hcp	33
	[$10\bar{1}0$]	3.79±0.1	sonics		
	[0001]	3.41±0.1			
Re	[$1\bar{2}10$]	3.50±0.1	ultra	hcp	32
	[$10\bar{1}0$]	3.00±0.1	sonics		
	[0001]	2.90±0.1			
Tl	[$1\bar{2}10$]	4.00±0.10	ultra-	hcp	34
	[$10\bar{1}0$]	4.00±0.10	sonics		
	[0001]	3.76±0.03			

B. Rhenium

The region of the Periodic Table occupied by the superconducting refractory metals is suitable for investigating the fundamental nature of energy-gap anisotropy. Extensive measurements have already been reported on niobium, a group-V transition metal with body-centered cubic (bcc) crystal structure.[16,17] The neighbors of Nb in the Periodic Table include Zr, a group-IV metal with hexagonal close-packed (hcp) structure; molybdenum, a group-VI metal with bcc structure; and rhenium, a group-VII metal with hcp structure. None of these has been investigated by tunneling for gap anisotropy. (For other methods on Re, see Table I.) We are systematically studying these metals in order to indicate the roles phonon spectra and electronic structure play, since for the above metals valence, crystal structure, and general band structure vary in a well-known fashion. With these considerations in mind, we have completed studies of Nb[16-18] and have undertaken a similar study of molybdenum in our laboratory.[19]

The Fermi surface calculated by Mattheiss has been successful in fitting with available data for rhenium from de Haas–van Alphen experiments.[20] As might be expected from its crystal structure (hcp) and valence (7), rhenium's Fermi surface is complicated and fragmented. Any meaningful matching of energy-gap values to the calculated topology would require a great supply of data. On the other hand, the phonon spectrum of rhenium is probably less complicated and similar to that of other hcp metals, some of which have been measured.[21]

C. Tunneling

As is seen in Table I, several methods of energy-gap measurement are available. Electron tunneling is the only one of these which provides a direct measurement of Δ. The energy gaps of superconducting electrodes separated by a tunneling barrier can be read from structure in the current-voltage characteristic of the electrode-barrier sandwich. According to a simple semiconductor model,[22] current across the barrier is proportional to the number of carriers free to tunnel, and the number of empty states available to receive them. This means that the current is dependent on the density of states in the superconductor. The superconducting density of states has sharp spikes near the gap edge, behaving as

$$\rho_s/\rho_n = |E|/(E^2-\Delta^2)^{1/2}\ .$$

It is this structure in the density of states which determines the current-voltage characteristic.

By introducing the possibility that Δ may be anisotropic we see that I-V curves taken for systematically oriented superconductor electrodes can give information on the variation of Δ. The derivative of such characteristics, (dI/dV)-V, makes analysis of the curves unambiguous, and provides a direct plot of the tunneling density of states as a function of energy measured from the Fermi level. (Second derivatives of I-V characteristics can reveal even 1% effects in the density of states.) Sample fabrication procedures are particularly important in tunneling experiments

TABLE II. Spectroscopic analysis of Cleveland Refractory Metals rhenium.

Al	8 ppm
Ca	1 ppm
Cr	5 ppm
Cu	1 ppm
Fe	50 ppm
Mb	1 ppm
Mn	1 ppm
Na	1 ppm
Mi	5 ppm
Si	5 ppm
Sn	1 ppm
O	0.0004 wt%
N	0.0010 wt%
H	0.0005 wt%
C	0.002 wt%

since the energy gap as measured near the metal surface in the sampling region of the current may be severely affected by the presence of defects or contaminants. Our fabrication procedure (see Sec. III A) minimizes surface contamination since the single crystals are grown in ultrahigh vacuum with no contact with any other materials, restrained only by their own surface tension, and they spend only about one monolayer time above room temperature. It is thought that the resulting surfaces may be structurally even more perfect than the interior of the material. The cylindrical geometry of our crystals allows several differently oriented tunneling junctions to be placed on the same sample, thus giving the anisotropy of the gap in a controlled manner, and allowing comparison with those obtained on other samples of possibly different metallurgical histories.

III. EXPERIMENTAL PROCEDURE

A. Sample Fabrication

Oriented single crystals of rhenium were grown in residual pressures of 10^{-9} Torr by the electron-beam floating-zone method. The $\frac{1}{8}$-in. -diam Re crystals were grown at the rate of 4 in./h from a rod obtained from Cleveland Refractory Metals, Solon, Ohio. Table II lists the impurities contained in this stock. Usually several passes were necessary, in combination with system bakeout, in order to achieve the desired pressure of 5×10^{-10}–5×10^{-9} Torr.

Resistivity ratios ($\rho_{300}/\rho_{4.2}$) were typically 1000 for our crystals; Table III lists specific values. The transition temperatures of the crystals were measured resistively to within 0.1% using a Wheatstone bridge together with a specially calibrated carbon resistor thermometer.

After growth, the Re crystals were removed from the ultrahigh vacuum system for sectioning into $1\frac{1}{4}$-in. -long sample lengths. The system was backfilled with pure nitrogen or oxygen prior to crystal removal, and sectioning was carried out in less than 5 min using a small, specially designed cutting wheel. The samples were then placed in another vacuum system and pumped to 10^{-6} Torr preparatory to fabrication of the tunneling barrier. Our experience showed that no insulating layer formed on the crystals during removal or sectioning in atmosphere. In fact, all efforts at oxidizing the surfaces in free-flowing oxygen at temperatures up to 150 °C proved to be fruitless. Junctions formed on such thermally oxidized rhenium surfaces showed the oxides to be good conductors in their own right. Rhenium forms many oxides and suboxides, such as Re_2O_7, ReO_3, and ReO_2. Although Re_2O_7 is insulating, it is difficult to achieve by gentle oxidation methods, and not dependable owing to its high solubility in water, alcohols, and other solvents.

Therefore, an artificial barrier was used by evaporating 20–50 Å of high-purity carbon onto the rhenium crystal surface. This layer was evaporated at the rate of 5 Å/sec in a vacuum of 10^{-6}–10^{-5} Torr by resistance heating of a narrowed region of a carbon rod, similar to conventional shadowing procedures used by electron microscopists.[23] An even layer of disordered carbon was ensured by motor-driven rotation of the crystal in the evaporation beam. Thickness measurements were made during evaporation by monitoring the frequency shift of a calibrated vibrating quartz-crystal microbalance.[24] Because the sensing head was not watercooled, careful preheating of the system or long cooling times before readings were necessary. Thicknesses were rechecked by interference measurements until a suitable familiarity with this procedure was achieved. Previous work has established that carbon films go down in a continuous manner on substrates of common metal films like copper, tin, and lead, and on niobium-crystal surfaces,[25] without requiring oxidation of

TABLE III. ρ_r (resistivity ratio) and T_c (transition temperature) of the samples of which successful tunneling measurements were done.

Crystal identification No.	Number of passes made for zone refining after bakeout	ρ_r	T_c (K=1%)	Transition width (K)
4	2	1340	1.717	0.020
7	2	3930	1.694	0.020
11	2	1160	1.696	0.004
14	2	740	1.691	0.006
18	2	1100	1.716	0.008
19	1	1150	1.716	0.008

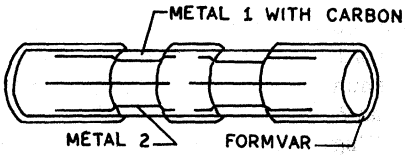

FIG. 1. Sample configuration. Metal 1 in our case is Re, and metal 2 is In.

the composite to "plug" up exposed metal at pinhole short-circuit sites common to semiconductor barriers such as CdS, ZnS, and germanium.

The samples were then removed from vacuum for a few minutes to allow suitable masking of the carbon-coated surface with Formvar to facilitate subsequent electrical connections. The samples were returned to the evaporator for deposition of counterelectrodes, usually indium, although silver was also used. The counterelectrodes were laid down as narrow stripes running the major part of the crystal's length, and located at desired orientations about the circumference. Stripe width was 0.010 in, corresponding to 9° subtended angle.

Electrical connections to the samples included a common current and a common voltage lead to the rhenium section, and two 0.005-in. -diam gold leads to each stripe. Thus several (1–4) Re-C-In junctions could be tested sequentially using four-point probe geometry. Figure 1 shows the resulting sample ready for testing.

B. Cryostat and Electronics

A conventional helium-4 Dewar assembly was used, with high-speed pumping. This system was capable of reaching 0.9 K. Resistivity ratio measurements, T_c values, and magnetic field and temperature dependences of the energy gap were taken in this cryostat. A typical transition temperature width is shown in Fig. 2. Temperature could be feedback controlled by an ac bridge technique[26] with a stability of 0.0001 K while taking data. Magnetic field was aligned parallel to the axis of the cylindrical crystals, and gap values taken point by point by changing the current in the solenoid.

Current-vs-voltage measurements and density-of-states–energy measurements of the junctions were taken by conventional techniques. For (dI/dV)-V plots, a small (< 70 μV peak to peak) ac sensing signal was superimposed on the dc signal, and the ac response of the junction was detected.

IV. RESULTS AND DISCUSSION

A. Crystal Cleanliness

Observation of energy-gap anisotropy requires that l/ξ_0 be somewhat greater than unity, where l is the electron mean free path, and ξ_0 is pair-coherence length defined in BCS theory. l/ξ_0 is given by

$$\sigma m k T_c/0.18\, hne^2 ,$$

where m is the electron rest mass, σ the conductivity, and n the net number of carriers. Mattheiss has recently published Fermi-surface information that provides the number of hole and electron carriers contributing to the conductivity.[27] Our own transition-temperature measurements are available in Table III. Schriemp has investigated the temperature dependence of conductivity in single-crystal rhenium of resistivity ratio 2490 from 2 to 20 °K,[28] allowing us to extrapolate 0 °K values of σ for crystals of different resistivity ratios. When we carry through this calculation, we find $l/\xi_0 \simeq 10$ for our crystals, well within the cleanliness regime required to observe gap anisotropy.

B. Junction Quality and Yield

No junctions were successful using thermal oxidation techniques to prepare tunneling barriers on rhenium single-crystal (or polycrystalline-wire) surfaces. Current-voltage characteristics of such junctions invariably showed nonlinear behavior unlike superconducting tunneling behavior, characteristic of both metallic-bridge shorts and direct-conduction processes. No superconducting-energy-gap structure was observable. In using an artificial barrier-fabrication technique, we were limited in sharpness of I-V characteristics by the nontunneling current contribution usually observed across disordered semiconducting carbon-film barriers due to direct or multistep conduction.[25,29] Because the surface oxides of rhenium are good conductors, it was not possible to use other semiconductor layers in combination with an oxidation step after Giaever to plug inherent "pinhole" shorts. The nontunneling current contributions did not seriously affect data gathering since the derivative technique used to obtain (dI/dV)-V curves made locations of significant structures in the data unambiguous. (The contribution might

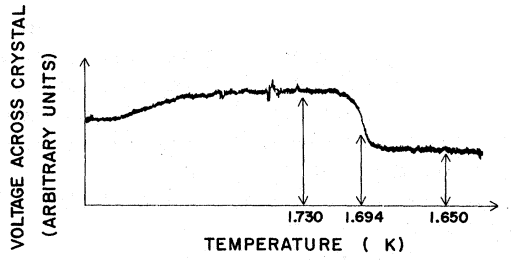

FIG. 2. Resistive transition by the four-point probe technique.

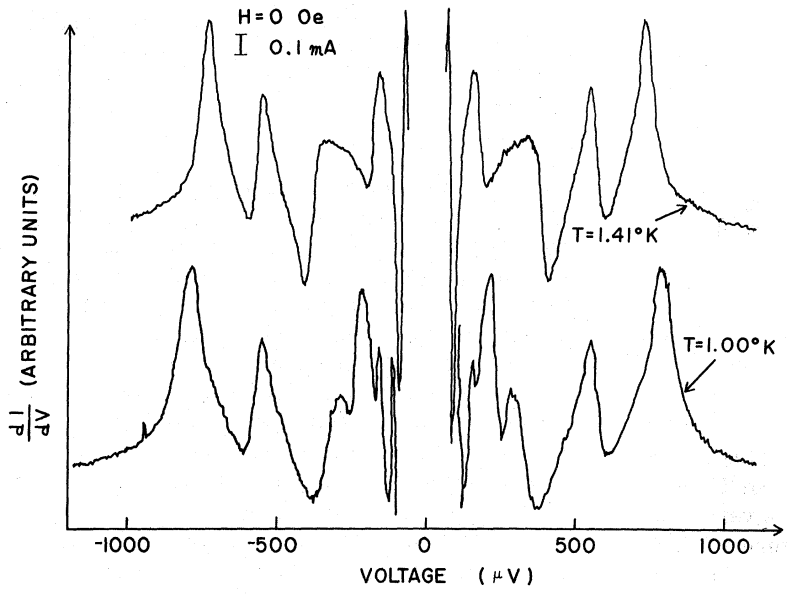

FIG. 3. Typical tunneling curves, dI/dV vs V.

become a disadvantage in studies of much weaker structures such as phonon spectra, where the absolute magnitude of the normalized density of states is desired and current shifts can affect phonon-energy measurements.) It is felt that alloys or compounds at the carbon-rhenium interface are unlikely in the conditions we use for fabrication, but little literature exists to corroborate this. About 10–15 % of the junctions yielded useful tunneling data.

C. Analysis

Gap-value determinations were done from structure in the (dI/dV)-V curves taken directly on the x-y recorder. These curves were swept continuously from negative to positive bias, affording a definitive zero. In one method of determination, the commonly taken double-particle conduction peak identified with rhenium, Δ_{Re}, was used directly to obtain rhenium energy-gap values. The second method used the corresponding double-particle structure for the second electrode, Δ_{In}, in combination with the sum peak $\Delta_{Re}+\Delta_{In}$ to determine Δ_{Re} values which could be compared to values obtained above. The second electrode, in the form of evaporated In stripes, was engineered to have an isotropic energy gap so as not to complicate the analysis: By maintaining a dirty evaporation vacuum, texturing was avoided,[30] and by keeping the thickness below a coherence length, $\xi_0 \sim 4400$ Å, double-gap values for Δ_{In} could not appear.[31]

A typical (dI/dV)-V plot is shown in Fig. 3.

D. Anisotropy Measurements

The values of the Re energy gap measured for nine crystallographic orientations are displayed in Fig. 4 on a conventional hcp stereographic triangle for the second (and most commonly used) method of analysis described above. (Hereafter these values of the energy gap are coded Δ^1_{Re} since they are determined from the single-particle sum peak.) These values of $2\Delta_{(0)}/kT_c$ range from 3.35 to 3.91 (±4%), with an averaged value of 3.59±4%, an anisotropy of 15.7%. Ultrasonic measurements for three main crystallographic directions have been made by Jones and Rayne.[32] They found values of 3.5±0.1 in the $[1\bar{2}10]$ direction; 3.01±0.1 in the $[10\bar{1}0]$ direction; and 2.9±0.1 in the [0001] direction. Comparison (where appropriate) to our data shows that their values run lower than ours. This is not unexpected, since an energy-gap value measured ultrasonically is a complicated average of all gaps associated with electrons sitting on the equatorial plane of the Fermi surface whose normals are normal to the wave propagator, and is dominated by effects of the smaller gaps.

Ultrasonic measurements of two other hcp metals, Zn[33] and Tl,[34] have been reported. The anisotropies observed in their respective superconduct-

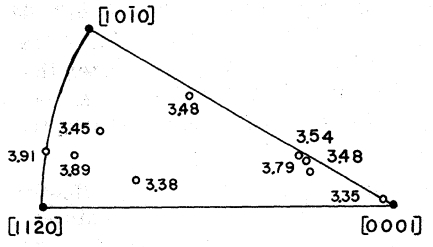

FIG. 4. Stereographic plot of energy-gap values determined from single-particle sum peak and double-particle indium structure; referred to in text as Δ^1_{Re}.

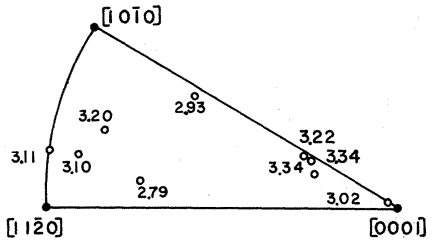

FIG. 5. Stereographic plot of energy-gap values determined from double-particle conduction peak for Re; referred to in text as Δ^2_{Re}.

ing energy gaps were in the same sense as for Re above, i.e., the [0001] direction having the smallest gap, and the [1$\bar{2}$10] direction having the largest. Since Zn has a valence of 2, Re of 7, and Tl of 3, the band structures of these metals are very different in spite of the same crystal structure and comparable Brillouin zones. The anisotropies suggest that instead of a dominant role being played by the electronic band structure, the phonon dispersion is responsible for gap anisotropy. When the phonon dispersions for hcp metals are examined, anisotropy in the spectrum is observed between the [0001] and [1$\bar{2}$10] directions, consistent with the above.[21] Bennett concluded from his calculations of energy-gap behavior in lead that the phonon dispersion is the basis of gap anisotropy.[13] Similarly, he showed that the gap behavior of single-crystal tin could be explained by its phonon dispersion.[11] This explanation was more consistent with the data observed than was the detailed Fermi-surface topology comparison Zavaritskii carried out.[10] A comparison of energy-gap data for Nb (of necessity less detailed) to its calculated Fermi surface showed little correlation of Δ to electronic structure.[16]

E. Double-Particle Peak Measurements and Selection Rules

Values of the rhenium energy gap determined directly from double-particle peaks of the same junctions as above are displayed in Fig. 5. (These values are noted as Δ^2_{Re} gaps since they are determined from structure ascribable to a double-particle tunneling process.) For every orientation, these values are smaller than the sum-peak values, Δ^1_{Re}, sometimes by as much as 25%. Further, Δ^2_{Re} values vary from $2\Delta_{(0)}/kT_c = 2.79 \pm 4\%$ to $3.34 \pm 4\%$, with an averaged value of $3.12 \pm 4\%$. This represents an anisotropy of 17.7%, greater than that for Δ^1_{Re}, and substantial disagreement of the sense of variation with that of Δ^1_{Re} and also with the ultrasonic data.

Observance of anisotropy in the single-particle tunneling energy gap rests on the existence of selection rules for wave functions coupling across the tunneling barrier.[35] In the case of an amorphous barrier such as our disordered carbon layers, the selection rule is that of zero transverse wave vector in the substrates repeated zone scheme; i.e., those electrons which penetrate the barrier are those whose WKB wave functions decay least across it. (Other selection rules exist, for instance, the preferential coupling that occurs if the barrier were epitaxial corresponds to an orientation-dependent selection rule.) There was no reason to suppose that double-particle tunneling selection rules should be different from those for single-particle tunneling. In that case, Δ^2_{Re} and Δ^1_{Re} values should be the same—in magnitude and anisotropy. Our measurements show that Δ^2_{Re} values do not correspond to Δ^1_{Re} values. Energy-gap structure consistent with a small second energy gap in Nb was recently analyzed from double-particle peaks.[18] These peaks, Δ^s_{Nb}, did not show anisotropy like that observed in the usual Nb gap. In fact, no anisotropy in Δ^s_{Nb} was observable. The Re and Nb data suggest that the double-particle tunneling process incorporates a selection rule which is different from the one usually supposed, and which is of averaged, or minimum, gap measured.

F. Temperature Dependence

The temperature dependence of the rhenium energy gap for a junction oriented near the [$\bar{2}$110] direction was reported earlier.[36] The behavior of $2\Delta_{(0)}/kT_c$ for this junction followed the BCS dependence calculated by Mühlschlegel[37] to within experimental error, over the temperature range $0.58 \leq t \leq 0.89$. Similar behavior is shown in Fig. 6 for a junction exhibiting both Δ^1_{Re} and Δ^2_{Re} values over the range $0.53 \leq t \leq 0.89$. This behavior is typical of all junctions studied, including that of one junction showing $2\Delta_{Re}/4$ peak structure, usually termed multiparticle or subharmonic structure.[38] Figure 6 shows the temperature dependences of Δ^1_{Re}, Δ^2_{Re}, Δ^4_{Re} of this junction for comparison. It is known that subharmonic structure, which appears when "weak links" exist across the barrier, requires invoking a slightly decreasing gap value Δ_n, as n increases in $2\Delta_n/n$, in order to analyze peaks in a consistent manner. Thus, the differences in $\Delta^4_{(0)}$, $\Delta^2_{(0)}$, and $\Delta^1_{(0)}$ magnitudes may be accounted for by this empirical procedure commonly known to "weak-link" investigators. However, the incompatibility of gap-anisotropy results is not resolvable.

G. Magnetic Field Dependence

The variation of the Re energy gap is shown in Fig. 7 for a junction determining both Δ^1_{Re} and Δ^2_{Re} gap values in its characteristics. The very sharp cutoff of the energy gap at the critical field is characteristic of bulk phenomenon, and sustains the validity of our anisotropy measurements. According to the particle model of Schrieffer and Wilkins,[39] the double-particle tunneling peak reflects the

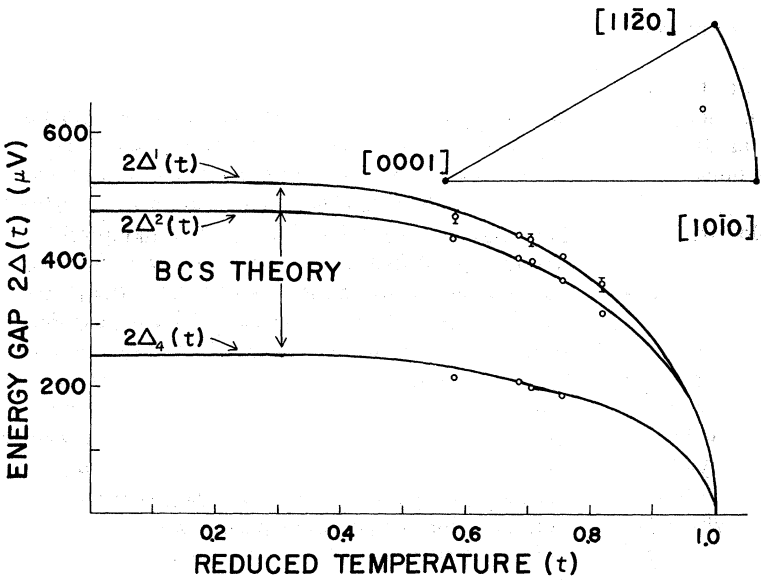

FIG. 6. Temperature dependence of Δ^1, Δ^2, Δ^4, where Δ^4 is data obtained from subharmonic structure.

quasiparticle density of states on only one side of the barrier (in the case of asymmetric junctions, S_A-I-S_B). Thus, application of a high enough magnetic field should affect the sum peak ($\Delta^1_{Re}+\Delta_{In}$), and any In double-particle peak, owing to field penetration of the In film before affecting Δ^2_{Re}. This procedure is useful to confirm identification of Re structure.

H. High-Bias Peak

On one occasion an additional second sum-peak structure was observed at a bias significantly higher (by ~ 1 meV) than the usual value. This (dI/dV)-V structure was of height and width comparable to the sum peak occurring at the expected value. We have observed similar structure for niobium-oxide-indium junctions on occasions[17] also at biases of approximately 1 meV beyond the sum peak. There was no systematic agreement of that structure with crystallography or fabrication procedures.

Recently Wyatt and Yelon[40] have observed structure above 2Δ in Pb-Pb junctions measured near

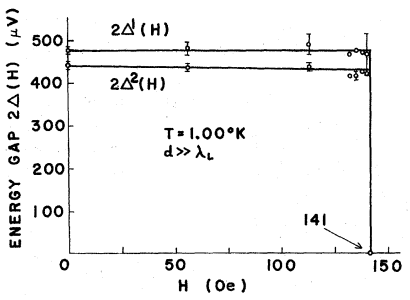

FIG. 7. Magnetic field dependence of Δ^1 and Δ^4.

T_c. As the temperature increased from 5 °K, the structure appeared and became larger. Such a structure is shown to be in agreement with BCS theory, resulting from the occupation of an appreciable number of states above the gap. Our data on Nb junctions were not taken near T_c, and our data on rhenium showed the existence of post-gap structure over a range well below T_c. Thus, it does not seem that the explanation of Wyatt and Yelon is related to our observations. Increasing the temperature toward T_c did not affect the sharpness of our structure, but led instead to the movement of the structure to *increasing* biases.

V. CONCLUSIONS AND SUMMARY

We have reported tunneling measurements in Re, made possible by utilizing an artificial-barrier technique. Anisotropy of the energy gap of clean superconducting single crystals was measured to be 15.7%. This anisotropy corresponds to reduced gap values of $3.35-3.91kT_c$ ($\pm 4\%$) observed over several crystal orientations. Our data were too sparse for a comparison to the rather involved rhenium Fermi-surface topology to be meaningful. However, no indication of multiple contributions to the sum peak was observed. Thus no evidence was seen that groups of electrons tunnel from different sheets of the Fermi surface and exhibit different Δ values as Zavaritskii reported for tin. Because the sense of the anisotropy from ultrasonic measurements made by other on rhenium, zinc, and thallium (all hcp metals, but is dissimilar valences) is the same, we suggest that gap anisotropies in these three metals do not depend significantly on the electronic band structures of the

metals, but are dominated by their similar phonon spectra.

Temperature-variation measurements of the energy-gap behavior show that the rhenium energy gap follows BCS dependence typical of weakly coupled superconductors at all orientations measured. Magnetic field measurements on the energy gap showed a sharp cutoff at the critical field, indicative of behavior dominated by the bulk rather than the surface effects that often plague tunneling-junction fabrication.

Values (Δ^2) for the rhenium energy gap determined from (dI/dV)-V structure commonly ascribed to double-particle tunneling showed temperature and magnetic field behavior similar to the values above determined by the more conventionally used "sum-and-difference" peak structures (Δ^1). However, the double-particle values did not reflect the same anisotropy as the former. Magnitudes of Δ^2 were always lower than Δ^1. Existing models for multiparticle tunneling do not include an explanation of decreased gap magnitudes, or different anisotropies. Selection rules for multiparticle tunneling different from those for single-particle tunneling might account for differing apparent anisotropies. However, it is difficult to conceive of physical reasons why wave-function matching at the barrier should vary in these two cases. A less contrived approach might entail examining the multiparticle-tunneling model itself, and what Δ means in that context. The Fermi surface and phonon spectrum may play different roles in double- and single-particle gap behavior. The Δ^1 and Δ^2 values for various crystallographic directions in rhenium suggest that if the roles *were* different in multiparticle tunneling, electronic structure must influence Δ^2 more significantly than Δ^1. Examining the multiparticle models will likely not lead to fundamental questions about the electronic-phonon influences, but rather to concerns of the barrier structure—such as uniformity, defect and impurity content, weak-link explanations, interface characterization, and related questions.

ACKNOWLEDGMENT

We gratefully acknowledge the aid of I. M. Puffer.

*Supported by the Office of Naval Research.

[1]R. W. Morse, T. Olsen, and J. D. Gavenda, Phys. Rev. Letters 3, 15 (1959).

[2]E. L. Dobbs and J. M. Perz, Rev. Mod. Phys. 36, 257 (1964).

[3]M. Levy, R. Kagiwada, and I. Rudnik, in *Proceedings of the Eighth International Conference on Low Temperature Physics, London*, 1962, edited by R. O. Davies (Butterworths, London, 1963).

[4]H. V. Bohm and N. H. Horowitz, in *Proceedings of the Eighth International Conference on Low Temperature Physics, London*, 1962, edited by R. O. Davies (Butterworths, London, 1963).

[5]N. H. Horowitz and H. V. Bohm, Phys. Rev. Letters 9, 313 (1962).

[6]R. David and N. H. Poulis, in *Proceedings of the Eighth International Conference on Low Temperature Physics, London*, 1962, edited by R. O. Davies (Butterworths, London, 1963).

[7]H. R. Hart and B. W. Roberts, Bull. Am. Phys. Soc. 7, 175 (1962).

[8]K. Yoshihiro and W. Sasaki, J. Phys. Soc. Japan 24, 426 (1968).

[9]J. Bardeen, L. N. Cooper, and J. R. Schrieffer, Phys. Rev. 108, 1175 (1957).

[10]N. V. Zavaritskii, Zh. Eksperim. i Teor. Fiz. 48, 837 (1965) [Sov. Phys. JETP 21, 557 (1965)].

[11]A. J. Bennett, Phys. Rev. 153, 482 (1967).

[12]G. I. Rochlin, Phys. Rev. 153, 513 (1967).

[13]A. J. Bennett, Phys. Rev. 140, A1902 (1965).

[14]B. L. Blackford and R. H. March, Phys. Rev. 186, 397 (1968).

[15]P. A. Bezuglyi, A. A. Galkin, and A. P. Korolyuk, Zh. Eksperim. i Teor. Fiz. 39, 7 (1960) [Sov. Phys. JETP 12, 4 (1961)].

[16]M. L. A. MacVicar and R. M. Rose, J. Appl. Phys. 39, 1721 (1968).

[17]M. L. A. MacVicar and R. M. Rose, Phys. Letters 26A, 510 (1968).

[18]J. W. Hafstrom and M. L. A. MacVicar, Phys. Rev. 186, 4511 (1969).

[19]M. Frommer (unpublished).

[20]L. F. Mattheiss, Phys. Rev. 151, 450 (1966).

[21]B. N. Brockhouse, in *Phonons and Phonon Interactions*, edited by T. A. Bak (Benjamin, New York, 1964).

[22]S. Shapiro, P. H. Smith, J. Nicol, J. L. Miles, and P. F. Strong, IBM J. Res. Develop. 6, 34 (1962).

[23]M. L. A. MacVicar, S. M. Freake, and C. J. Adkins, J. Vac. Sci. Technol. 6, 717 (1969).

[24]B. W. Kington, Marconi Instr. 10, 81 (1964).

[25]M. L. A. MacVicar, J. Appl. Phys. 41, 4765 (1970).

[26]G. A. Beske, Sc. D. thesis (MIT, 1965) (unpublished).

[27]L. F. Mattheiss (unpublished).

[28]J. T. Schriemp, J. Phys. Chem. Solids 28, 2581 (1967).

[29]I. Giaever, Phys. Rev. Letters 20, 1286 (1968).

[30]H. L. Caswell, J. Appl. Phys. 32, 2641 (1961).

[31]C. K. Campbell and D. G. Walmsley, Can. J. Phys. 45, 159 (1967).

[32]C. K. Jones and J. A. Rayne, Phys. Letters 21, 510 (1966).

[33]M. F. Lea, J. D. Llewellyn, D. R. Peck, and E. R. Dobbs, in *Proceedings of the Eleventh International Conference on Low Temperature Physics*, edited by J. F. Allen *et al.* (St. Andrews U. P., St. Andrews, Scotland, 1969).

[34]G. A. Sanders and A. W. Lawson, Phys. Rev. 135, A1161 (1964).

[35]J. E. Dowman, M. L. A. MacVicar, and J. R. W Waldram, Phys. Rev. 186, 452 (1969).

[36]S. I. Ochiai, M. L. A. MacVicar, and R. M. Rose, Solid State Commun. 8, 1031 (1970).

[37]B. Mühlschlegel, Z. Physik 155, 313 (1959).
[38]J. M. Rowell and W. L. Feldman, Phys. Rev. 172, 393 (1968).
[39]J. R. Schrieffer and J. W. Wilkins, Phys. Rev. Letters 10, 17 (1963).
[40]P. W. Wyatt and A. Yelon, Phys. Rev. (to be published).

PHYSICAL REVIEW B VOLUME 4, NUMBER 9 1 NOVEMBER 1971

Superconductivity and Magnetic Scattering in La-Ce†

J. J. Wollan* and D. K. Finnemore‡
Institute for Atomic Research and Department of Physics, Iowa State University, Ames, Iowa 50010
(Received 30 April 1971)

Magnetic impurity scattering for La-Ce has been studied for temperatures well below both the superconducting transition temperature and the Kondo temperature. Two different spin scattering times are involved in this problem. The spin scattering time associated with the breaking of Cooper pairs is found to be approximately 5×10^{-11} sec and to be nearly independent of temperature. The spin scattering time associated with the Kondo effect, however, is found to be on the order of 10^{-14} sec and to have a very strong temperature dependence. These two scattering times appear to be independent of one another. A thorough study of the negative magnetoresistance is presented for several values of impurity concentration to help unravel the effects of impurity-impurity interactions.

I. INTRODUCTION

Magnetic impurity states in metals have been studied[1-4] extensively in the past few years and the experimental evidence seems to confirm the fundamental ideas presented by Anderson[5] for the formation of the impurity ground state. Within this model the formation of a local moment on an impurity site depends on the relative magnitude of the intra-atomic Coulomb repulsion, U, between two electrons of opposite spin, and the broadening Δ caused by the mixing of the impurity state with the conduction band. Large U compared to Δ favors a magnetic ground state, and large Δ compared to U favors a nonmagnetic ground state. Another feature of the model is that the exchange coupling constant of the Heisenberg Hamiltonian, J, is also controlled by the strength of the mixing, V_{kf}.[6] For small V_{kf} the ordinary atomic exchange integral dominates and J is positive (ferromagnetic coupling), whereas for large V_{kf} the mixing term dominates and J is negative (antiferromagnetic coupling).[6] Both the superconducting- and the normal-state properties of the material depend on the values of U, Δ, and V_{kf}, and it is often convenient to categorize the alloy according to the relative magnitude of these parameters.

From a theoretical point of view, the easiest case to solve is that of very weak mixing (small V_{kf}), where $U\gg\Delta$, J is positive, the magnetic impurities are paramagnetic, and the spin scattering time for breaking Cooper pairs, τ_s, is independent of temperature. Abrikosov and Gor'kov[7] have determined the superconducting behavior for this kind of impurity, and the calculations for the free energy and the thermal conductivity[8,9] agree with the experimental work on Th-Gd to an accuracy of a few percent.

For the case of strong mixing (large V_{kf}) the problem is more difficult. Here U is approximately equal to Δ, J is negative, the impurity ground state is nonmagnetic, and localized spin flucuations are an important factor.[10] Experimental work such as the studies of Al-Mn[11] and Th-U[12] seem to confirm the qualitative aspects of localized spin fluctuations,[10] but quantitative verification is not yet available.

La-Ce alloys are a rather special case in that the mixing strength is intermediate between the above two extremes.[6] For these alloys V_{kf} is strong enough to give a negative J and yet weak enough to give a well defined moment ($U/\pi\Delta\sim5$). Hence it is one of the few systems to show a Kondo effect and still have U substantially greater than $\pi\Delta$.

A long series of experimental and theoretical studies have domonstrated the superconducting and Kondo-like properties of La-Ce at temperatures near or above the Kondo temperature. Sugawara and co-workers[13] first reported the presence of a resistance minimum and showed the effect it might have on the superconducting critical-field curves. Soon afterward, Edelstein[14] and Culbert and Edelstein[15] carried out electron tunneling and specific heat measurements to look for magnetic impurity states in the superconducting energy gap. In addition to this work, Maple and co-workers[16] have presented convincing experimental evidence that the position of the $4f$ level and the strength of the interaction parameters can be varied by the application